

Article

## Trans and surface membrane bound zervamicin IIB: $^{13}\text{C}$ -MAOSS-NMR at high spinning speed

J. Raap<sup>a,\*</sup>, J. Hollander<sup>a</sup>, T. V. Ovchinnikova<sup>b</sup>, N. V. Swischeva<sup>b</sup>, D. Skladnev<sup>c</sup> & S. Kiihne<sup>a</sup>

<sup>a</sup>Leiden Institute of Chemistry, Leiden University, P.O. Box 9502, 2300 RA, Leiden, The Netherlands;

<sup>b</sup>Shemyakin & Ovchinnikov Institute of Bioorganic Chemistry, Moscow, Russia; <sup>c</sup>State Research Institute of Genetics and Selection of Industrial Microorganisms, Moscow, Russia

Received 23 February 2006; Accepted 21 June 2006

**Key words:** peptide antibiotic, solid state  $^1\text{H}$ -,  $^{13}\text{C}$ -,  $^{31}\text{P}$ -NMR, substrate supported PC10 and POPC bilayers

### Abstract

Interactions between  $^{15}\text{N}$ -labelled peptides or proteins and lipids can be investigated using membranes aligned on a thin polymer film, which is rolled into a cylinder and inserted into the MAS-NMR rotor. This can be spun at high speed, which is often useful at high field strengths. Unfortunately, substrate films like commercially available polycarbonate or PEEK produce severe overlap with peptide and protein signals in  $^{13}\text{C}$ -MAOSS NMR spectra. We show that a simple house hold foil support allows clear observation of the carbonyl, aromatic and  $\text{C}^\alpha$  signals of peptides and proteins as well as the ester carbonyl and choline signals of phosphocholine lipids. The utility of the new substrate is validated in applications to the membrane active peptide zervamicin IIB. The stability and macroscopic ordering of thin PC10 bilayers was compared with that of thicker POPC bilayers, both supported on the household foil. Sidebands in the  $^{31}\text{P}$ -spectra showed a high degree of alignment of both the supported POPC and PC10 lipid molecules. Compared with POPC, the PC10 lipids are slightly more disordered, most likely due to the increased mobilities of the shorter lipid molecules. This mobility prevents PC10 from forming stable vesicles for MAS studies. The  $^{13}\text{C}$ -peptide peaks were selectively detected in a  $^{13}\text{C}$ -detected  $^1\text{H}$ -spin diffusion experiment. Qualitative analysis of build-up curves obtained for different mixing times allowed the transmembrane peptide in PC10 to be distinguished from the surface bound topology in POPC. The  $^{13}\text{C}$ -MAOSS results thus independently confirms previous findings from  $^{15}\text{N}$  spectroscopy [Bechinger, B., Skladnev, D.A., Ogral, A., Li, X., Rogozhkina, E.V., Ovchinnikova, T.V., O'Neil, J.D.J. and Raap, J. (2001) *Biochemistry*, **40**, 9428–9437]. In summary, application of house hold foil opens the possibility of measuring high resolution  $^{13}\text{C}$ -NMR spectra of peptides and proteins in well ordered membranes, which are required to determine the secondary and supramolecular structures of membrane active peptides, proteins and aggregates.

### Introduction

Presently, the method of Magic Angle-Oriented Sample Spinning (MAOSS) can be applied to

study the structure and dynamics of lipids, peptides and proteins in a membrane environment by application of mechanically orientated samples of lipid bilayers. Samples of uniaxially aligned lipid molecules in multilamellar membranes are usually prepared on glass plates, which are stacked on top

\*To whom correspondence should be addressed. E-mail: J.Raap@chem.LeidenUniv.nl

of each other inside a 7 mm rotor (Glaubitz and Watts, 1998). Magic angle spinning at just a few kHz, in combination with the fast axial diffusion of lipid molecules, is already sufficient to average the dipolar couplings of hydrogen nuclei. In this manner spinning side bands in the  $^1\text{H}$ -NMR spectrum are removed, leading to a reduction of signal overlap and increase in the primary signals up to the sensitivity and resolution of solution NMR spectra (Forbes et al., 1988; Halladay et al., 1990). For membrane bound  $^{15}\text{N}$ - and  $^2\text{H}$ -labelled peptides and proteins, the resolution of the  $^{15}\text{N}$  and  $^2\text{H}$ -NMR spectra can also be enhanced through reduction of the chemical shift and quadrupolar anisotropies of these nuclei (Marassi et al., 1997; Glaubitz, 2000). Another advantage of the substrate supported MAOSS technique is that short chain di-C10:0-PC (PC10) lipids, which do not self-assemble to vesicles in aqueous solution, are stabilized as multilamellar bilayers at the glass surface (Bechinger et al., 2001). The method, however, exhibits a few serious disadvantages. To avoid movement of the lipid towards the edges of the glass plates, due to centrifugal forces, the method is restricted to measurements at low spinning speeds. Due to the relatively heavy weight of the stack of glass plates, inserted in a 7 mm rotor, samples are difficult to spin at constant, high spinning speeds. Since, glass plates occupy most of the volume of the NMR rotor, only little amounts of the compound of interest can be studied.

Another problem arises for NMR measurements at ultra-high magnetic fields. In this case, the advantage of the increased sensitivity at high magnetic fields is counter-balanced by the disadvantage of the increased spread of spinning side bands. For averaging of the large chemical shift anisotropies (CSA) of amide and aromatic  $^{13}\text{C}$ -atoms of the more rigidly membrane-bound peptides or proteins, very high spinning speeds are necessary to obtain a high resolution spectrum at the desired sensitivity. This problem is even more serious for measurements of  $^1\text{H}$  nuclei of peptides and proteins. In this case the line broadening mainly caused by dipolar couplings cannot be sufficiently averaged at spinning speeds equal or less than 11 kHz. This practical problem has been solved for  $^{15}\text{N}$ - and  $^{31}\text{P}$ -MAOSS-NMR measurements at high spinning speeds by means of a preparation of membranes with the long axis of the lipid oriented perpendicular to the rotation

axis (Bechinger et al., 2001; Sizun and Bechinger, 2002). This was achieved by preparation of a multilamellar membrane on the surface of rolls of thin films of PolyEtherEtherKetone (PEEK) or polycarbonate.

Since we are interested in  $^{13}\text{C}$ -MAOSS-NMR measurements of  $^{13}\text{C}$ -labelled membrane bound peptides we first measured the  $^{13}\text{C}$  spectrum of commercially available polycarbonate foil. It is found, however, that this material contains anti-flammable aromatic compounds. Thus, the presence of aromatic signals in the  $^{13}\text{C}$ -NMR spectra of foils of polycarbonate as well as in the aromatic thermoplast PEEK hamper the study of aromatic side chains of amino acid residues of peptides and proteins. Another recently reported method is based on the technique of substrate-supported lipid nanotube arrays. In this technique phospholipid molecules self-assemble to membranes inside the rather large surface of cylindrical nanopores, oriented parallel to the NMR rotor, and assembled on a stack of cylindrical anodic aluminium disks (Smirnov and Poluektov, 2003; Wattraint and Sarazin, 2005).

In the present paper we describe the utility of a new substrate that allows to measure high resolution  $^{13}\text{C}$ -MAOSS-NMR spectra at the amide, aromatic and  $\text{C}^\alpha$  regions for samples of  $^{13}\text{C}$ -labelled peptides and proteins even in membranes which would otherwise not be stable. Simple house hold foil, that can be easily obtained from local super markets and which is generally used to wrap up food, is found the material of choice to stabilize even membranes composed of short chain PC10 lipids. Parameters describing the degree of alignment of PC10 lipid molecules at this foil are compared with those of POPC. It will be shown that substrate aligned membranes are stable up to the spinning speed of 11 kHz. The application of this foil-supported membrane system in  $^{13}\text{C}$ -MAOSS investigations was tested by the study of different binding modes of the membrane active peptide ( $^{13}\text{C}$ -labelled) zervamicin IIB. This peptide was chosen due to the fact that, according to a recent static solid state  $^{15}\text{N}$ -NMR study of ( $^{15}\text{N}$ -labelled) zervamicin IIB, reconstituted on glass plate aligned membranes, the orientation of this peptide can be controlled dependent on the thickness of the phospholipid membrane (Bechinger et al., 2001). In thick bilayers (composed of POPC lipid molecules) the long axis of this peptide

helix is oriented parallel to the surface, whereas in thin bilayers (short chain PC10 lipids) its backbone adopts the transmembrane orientation. In the present report the presence of perpendicular and parallel binding states in thin and thick house hold foil supported membranes is confirmed by the results of a  $^{13}\text{C}$ -detected  $^1\text{H}$ -spin diffusion experiment to separate the  $^{13}\text{C}$  signals of the peptide from the overlapping natural abundance lipid peaks (Huster et al., 2002) and by analysis of the spin diffusion build-up curves.

## Materials and methods

### Materials

PC10 (MW 565.7) and POPC (MW 760.1) were purchased from Sigma (UK). [ $^{13}\text{C}$ ]-zervamicin was prepared as described elsewhere (Ovchinnikova et al., 2003). The primary structure of this linear hexadeca peptide is characterized by an N-terminal acetyl group, a C-terminal 1,2-aminoalcohol and the presence of proteinogenic as well as non-DNA coded tetra-substituted amino acids, like  $\alpha$ -aminoisobutyric acid and D-isovaline. The sequence is AcTrp-Ile-Gln-Iva-Ile<sup>5</sup>-Thr-Aib-Leu-Aib-Hyp<sup>10</sup>-Gln-Aib-Hyp-Aib-Pro<sup>15</sup>-Phl (Hyp, 4-hydroxyproline; Phl, L-phenylalaninol) (Krishna et al., 1990). Its 3D structure (Baloshova et al., 2002; Shenkarev et al., 2002) as well as its channel properties (Agarwalla et al., 1992; Balaram et al., 1992; Sansom et al., 1993) were reported earlier. 'Paclan' house hold foil, also sold under the commercial names 'Perfect', 'Markant' and 'AH Huishoudfolie', was purchased at a local super market. This hydrophilic film is produced by CeDo Household Products Ltd. Telford, UK by co-polymerization of a 3:1 mixture of ethylene and butene to which 0.02% glycerol monooleate was added during the process to make the film wettable. According to elemental analysis, the foil consists of 85.66% carbon, 15.67% hydrogen and a trace of 0.92% sulphur (the nitrogen content was beyond detection limit).

### Preparation of oriented bilayers

To cover the total surface area with a thin and homogeneous layer of lipid, a co-solution of 2 mg of uniformly  $^{13}\text{C}$ -labelled (99%) zervamicin (MW

1947) and 40 mg PC10 (molar ratio P:L = 1:70) in 0.5 ml of trifluoroethanol was transferred with a syringe to a horizontal oriented film ( $30 \times 1.5$  cm). The sample solution was spread by slowly moving the syringe needle with simultaneous evaporation of the solvent by a stream of nitrogen gas. The last traces of solvent were removed by keeping the sample in vacuum for one night at room temperature. Hydration of the multilamellar bilayers in the liquid crystal phase was achieved by spraying the surface with a fine mist of pure water (or buffer). Finally, the membrane loaded film was rolled-up and inserted into a 4 mm rotor (internal diameter 3 mm). The roll does not occupy the total volume of the MAS-NMR rotor and a cylindrical hole remains inside. The same method was used for the sample preparation of labelled zervamicin bound to POPC (2 mg/40 mg), but due to the insolubility of POPC in pure trifluoroethanol, ethyl acetate was added up to a final content of 70%. Tentative assignments of  $^{13}\text{C}$  NMR signals of zervamicin were based on high resolution NMR data of zervamicin IIB in methanol solution (Balashova et al., 2002). Proton resonances of PC10 lipid were assigned by using the spectral information obtained from a 2D-HSQC spectrum of a sample of PC10 lipid in  $\text{CDCl}_3$ .  $^1\text{H}$  and  $^{13}\text{C}$ -NMR assignments of POPC were taken from the literature (Gaede and Gawrisch, 2004).

### NMR experiments

All experiments were carried out using a Bruker AV-750 MHz spectrometer, equipped with a double channel cross polarization (CP)-MAS probe head running with a spinning speed of 11 kHz, unless indicated elsewhere. 1D  $^{13}\text{C}$ -NMR spectra were recorded at a spectrometer frequency of 188 MHz with both Hahn-echo and CP pulse schemes. The  $^{13}\text{CO}$  resonance of [ $^{13}\text{C}$ ]-tyrosine-HCl at 172.1 ppm was used as an external reference to determine the isotropic chemical shifts relative to TMS.  $^{31}\text{P}$  spectra of the lipid membranes were recorded at 303 MHz.  $^{13}\text{C}$ -detected  $^1\text{H}$  spin diffusion MAOSS spectra were recorded using the conditions used in the group of Prof Mei Hong and described in (Huster et al., 2002), but using a standard cross polarization pulse sequence for the transfer of magnetization of  $^1\text{H}$  to  $^{13}\text{C}$ . The CP contact time used was 512  $\mu\text{s}$ . A Goldman-Shen (Goldman and Shen, 1966)  $T_2$  filter (1.96 ms)

was applied to selectively excite the more mobile lipid protons. Experiments were run for different spin diffusion mixing times  $\tau_m$  (5–145 ms). The number of scans used to record the spectra was 320 with a digital resolution of  $1\text{TD} = 120$  (60 real and 60 imaginary data points). 2D Fourier transformation was achieved with  $S11 = 1024$  for the proton dimension and  $S12 = 2048$  for the  $^{13}\text{C}$  dimension. All 2D spectra were measured *in duplo* using freshly prepared samples.  $T_1$  values of different lipid protons were measured in a standard inversion-recovery experiment: choline methyl (515 ms, POPC; 760 ms, PC10) and  $\omega$ -methyl protons (1124 ms, POPC; 930 ms, PC10). Spin diffusion build-up curves were simulated by using the program based on a 1D lattice model (Huster et al., 2002). Spin diffusion rates were calculated using spin diffusion coefficients  $0.042\text{ nm}^2/\text{ms}$  (intramolecular spin diffusion  $D_L$  of lipid chain protons),  $0.0088\text{ nm}^2/\text{ms}$  (intermolecular transfer between lipid and peptide protons  $D_{L/P}$ ) and  $0.25\text{ nm}^2/\text{ms}$  (intramolecular spin diffusion of peptide protons  $D_P$ ). The value of  $D_P$  was taken from the literature (Huster et al., 2002). The values of  $D_L$  and  $D_{L/P}$  were obtained by fitting the experimental data obtained for the choline methyl protons of PC10. The following geometrical parameters were used: (1) distance between vicinal protons 0.2 nm, (2) shortest lipid–peptide distance 0.2 nm and (3) length of the long axis of peptide helix 2.9 nm.

### *Simulation of $^{31}\text{P}$ spectra*

Oriented MAS  $^{31}\text{P}$  spectra were simulated using a home made program in Matlab (version 7.0.4). Briefly, this program calculates the expected MAS side band pattern for an axially symmetric (motional averaged)  $^{31}\text{P}$  tensor at a particular nominal orientation with respect to the rotor axis (e.g.  $90^\circ$  or  $0^\circ$ ) rotating at the magic angle with respect to the main magnetic field. The method is closely based on the description found in reference (Eden and Levitt, 1998). Significant mosaic spread is accounted for by calculating 500 spectra for  $\beta$ -orientations distributed over a range covering the nominal alignment  $\pm 5$  times the estimated mosaic spread. The  $\alpha$ -angles for these spectra are chosen randomly and the  $\gamma$  values are set to  $0^\circ$ . To calculate the final spectrum, the 500 ‘oriented’ spectra are multiplied by weighting factors corresponding

to a Gaussian distribution centred at the nominal alignment angle, summed, and normalized. A separate spectrum is calculated for an isotropically oriented component of the sample using 256 distributed crystallite orientations [‘256 step hemi’ from reference (Eden and Levitt, 1998)]. This isotropic component is then weighted and summed with the oriented spectrum obtained from the Gaussian distribution of  $\beta$ -angles. The resultant simulated spectrum is normalized and Lorentzian broadening is applied. The  $\chi$ -squared value between the simulated and experimental spectra is minimized using a simplex minimization routine as implemented by the `fmins` command in Matlab, while allowing the nominal alignment angle, the fraction isotropic signal, the mosaic spread, and the Lorentzian broadening to vary freely. Additional user adjustments of the isotropic chemical shift, spin rate, and chemical shift anisotropy are usually required to obtain optimal fits.

## **Results**

### *$^{31}\text{P}$ MAOSS-NMR*

To analyse the degree of lipid alignment (or at least the order of the phospholipid headgroups)  $^{31}\text{P}$ -NMR spectra of oriented lipid samples were recorded at different spinning speeds. In Figure 1, for example, the experimental and simulated orientation-dependent side band patterns are shown for membranes of POPC (A) and PC10 (B), loaded on the house hold foil and obtained at 1.5 kHz. Addition of peptide to the lipid membrane does not influence the shape of the patterns, indicating that the presence of peptide does not perturb the overall membrane orientation. The stability of the sample during spinning was checked by a comparison of spinning side band spectra measured at 1.5 kHz before and after spinning at 11 kHz. Excellent agreement was found for the measured and simulated spinning side band patterns at different spinning speeds. Parameters of the simulated spectra are listed in Table 1. For POPC lipid molecules, a high degree of alignment was found for the substrate supported multilamellar bilayers in the liquid crystal phase. For PC10 lipid molecules, the ordering is apparently lower as is reflected by the increased mosaic spread and isotropic fraction. It is plausible that ordering of

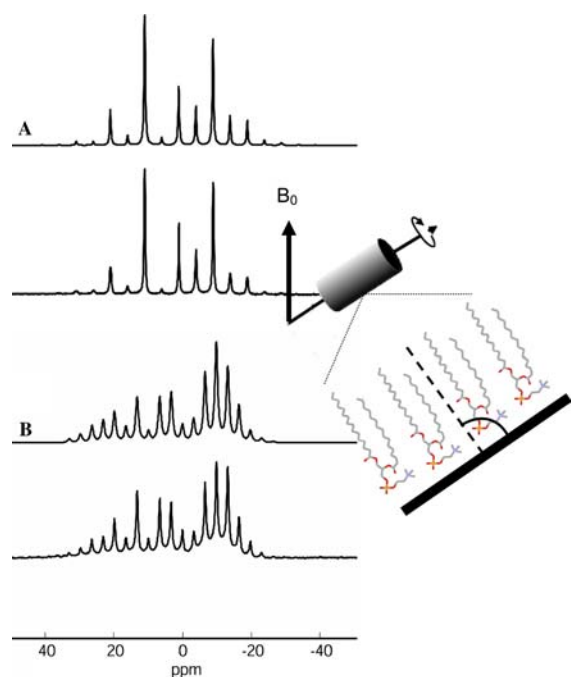


Figure 1. 750 MHz  $^{31}\text{P}$ -MAOSS spectra recorded at 298 K and spinning rate of 1.5 kHz about the magic angle for POPC (A) and PC10 (B) with the long lipid axis making an angle  $\beta$  with the rotor axis. The simulated spectra are shown above for comparison. The cartoon demonstrates the sample geometry.

the headgroups is affected by the increased mobility of the short chain lipid molecules.

### $^1\text{H}$ MAOSS-NMR

Spectra of zervamicin bound to the PC10 membrane, depicted in Figure 2, illustrate that the spinning side bands of the lipid proton signals (line width 100 Hz) are almost removed by spinning the sample at a speed of 3 kHz.  $^1\text{H}$  chemical shifts of the different lipid protons (ppm values are given within brackets) were assigned to  $\text{CH}_2$  (5.3),  $\text{CH}_{1,3}$  (4.5),  $\beta$  (4.0–4.3),  $\alpha$  (3.6),  $\text{N}(\text{CH}_3)_3$  (3.4),

$\text{NCH}_2$  (2.3),  $(\text{CH}_2)_n$  (1.3–1.6) and  $\text{CH}_3-\omega$  (1.0). The signals of the house hold foil polymer  $(\text{CH}_2)_n$  overlap with the lipid peaks at 1.3–1.6 ppm. Due to the low concentration of peptide, the aromatic proton signals are not detected (see inset).

The MAOSS spectrum of the POPC membrane (not shown) was characterized by the assignments of the lipid protons, i.e. oleoyl  $\text{CH}_{9,10}$  (5.3),  $\text{CH}_2$  (4.7),  $\text{CH}_{1,3}$  (4.5),  $\beta$  (4.3),  $\alpha$  (4.0),  $\text{N}(\text{CH}_3)_3$  (3.4),  $\text{NCH}_2$  (2.7),  $\text{CH}_2\text{CO}$  (2.5, 2.3, and 2.1),  $(\text{CH}_2)_n$  (1.3–1.6) and  $\text{CH}_3-\omega$  (1.0).

### $^{13}\text{C}$ MAOSS-NMR

Figure 2 (top) shows the Hahn-echo 1D  $^{13}\text{C}$ -MAOSS spectrum of  $[\text{U}-^{13}\text{C}]$ -zervamicin/PC10 recorded at 313 K and a spinning speed of 11 kHz. Except for the signals of the aromatic side chains of  $\text{Trp}^1$  and  $\text{Phe}^{16}$  shown at the 112–132 ppm region, the other peptide resonances severely overlap the natural abundance signals of the lipid. The regions 170–180, 48–65, and 10–48 ppm are typical for  $^{13}\text{C}$  resonances of the following carbon atoms: (1) lipid ester carbonyl and peptide amide carbonyl, (2) peptide  $\text{C}^\alpha$ , lipid choline  $\text{C}^\alpha$ ,  $\text{C}^\beta$  as well as C1, C2 and C3 of the glycerol moiety and (3) other side chain carbon atoms of lipid and peptide. The carbon peaks of the polymer, a singlet at 32.1 ppm with a shoulder at 30.3 ppm, are hidden by the signals of the aliphatic carbon atoms of both lipid and peptide (Figure 3).

In spite of the high  $^{13}\text{C}$ -enrichment (99%) of the peptide, the intensities of the aromatic signals are lower than those of the natural abundance peaks of the lipid.

The lower intensities of the peptide lines are caused by differences between the line widths of peptide (350 Hz) and lipid (175 Hz) as well as by the 70-fold molar excess of lipid. The cross polarization spectrum depicted at the bottom of Figure 2 shows a slightly better resolution of the

Table 1. Chemical shift anisotropy parameters of oriented lipid membranes

Lipid	CSA			Results of fitting	
	$\delta$ (ppm)	$\eta$	$\beta$ (degrees)	Mosaic spread ( $\Delta\beta$ ) (degrees)	Isotropic fraction (%)
POPC	39	0	88	5	0
PC10	32	0	95	22	10

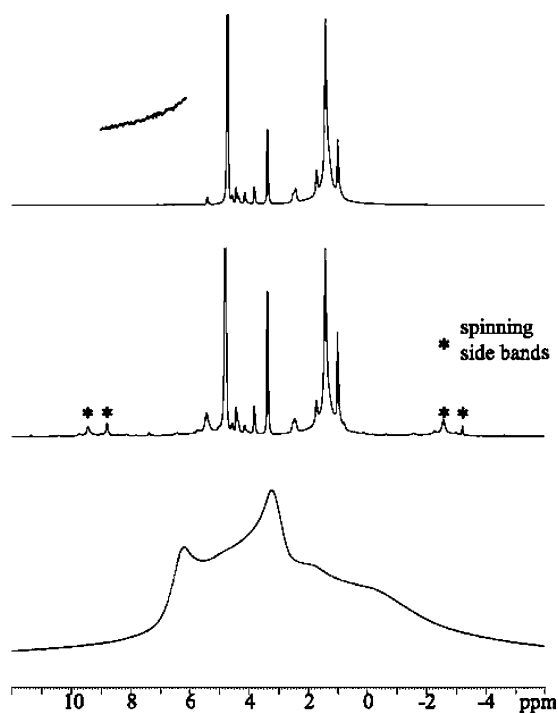


Figure 2. 750 MHz  $^1\text{H}$ -MAOSS spectra recorded at 313 K of zervamicin bound to the PC10 membrane (molar ratio of peptide:lipid = 1:70) at spinning speeds of 11 kHz (top), 3 kHz (middle) and 0 kHz. The insert of the upper spectrum at the noise level indicates that aromatic proton signals of Trp<sup>1</sup> and Phe<sup>20</sup> are not detected at this peptide to lipid ratio.

peptide signals, particularly in the 48–65 ppm and 10–15 ppm regions, due to the decreased intensities of overlapping lipid resonances. The combined phenomena of cross polarization and the difference between the mobilities of lipid and peptide molecules form the basis of the complete removal of the lipid signals in the spin diffusion experiment.

#### $^{13}\text{C}$ -detected $^1\text{H}$ -spin diffusion MAOSS-NMR

For protein channels bound to vesicular membranes it was possible to remove the lipid  $^{13}\text{C}$ -signals from the overlapping protein peaks by application of a  $^{13}\text{C}$ -detected  $^1\text{H}$ -spin diffusion technique (Kumashiro et al., 1998; Huster et al., 2002). The applied pulse scheme, briefly described here, starts with a  $T_2$  filter (Goldman and Shen, 1966), which enables the selective excitation of proton spins of the relatively mobile lipid molecules. In the next step, the magnetized spins are allowed to diffuse along pathways, mainly determined by differences between dipolar couplings of

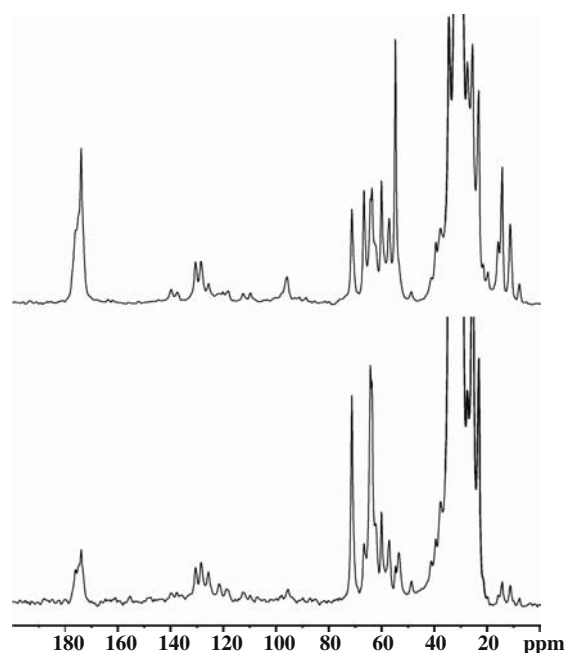
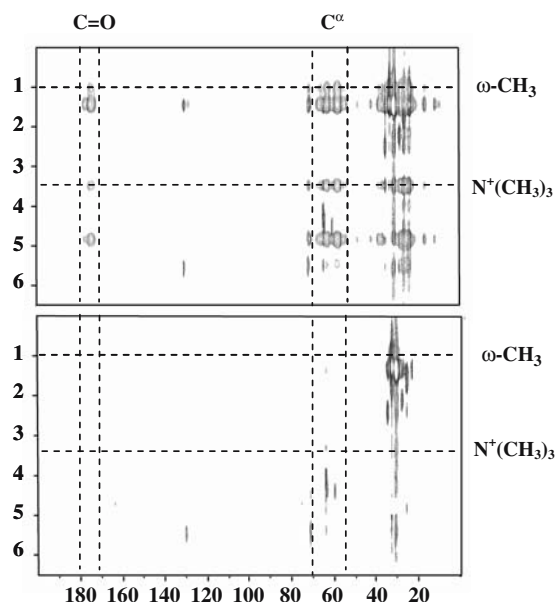


Figure 3. 750 MHz 1D- $^{13}\text{C}$ -MAOSS spectra of the [ $^{13}\text{C}$ ]-zervamicin/PC10 sample recorded with Hahn-echo (top) and CP (bottom) pulse schemes. The asterisk indicates a spinning side band of the large polymer peak at 32.1 ppm.

neighbouring lipid protons. The rate limiting step is the transfer of magnetization from lipid to peptide protons, which is dependent on the inter-atomic distance. After this step, the magnetization of the proton spins is rapidly equilibrated to all other protons of the more rigid peptide molecule due to their larger dipolar couplings. In the final cross polarization step proton magnetization is transferred to the  $^{13}\text{C}$ -spins of the peptide atoms and detected. Analysis of the spin-diffusion build-up curves from the lipid  $\omega$ -methyl protons to the aliphatic side chain protons, detect the  $^{13}\text{C}$  protein intensities, yields information about the degree of insertion of the peptide within the lipid bilayer. Since the insertion should be different for perpendicular and parallel orientations of zervamicin in thin and thick membranes, this technique was chosen to test the utility of our substrate supported membrane system for investigation of the topology of membrane active peptides and proteins.

The  $^{13}\text{C}$  detected  $^1\text{H}$ -diffusion-MAOSS NMR spectrum of uniformly labelled zervamicin in POPC bilayers was recorded at 298 K (upper panel of Figure 4) with a spin diffusion mixing time  $\tau_m$  of 145 ms. The lower temperature was chosen



**Figure 4.** 2D  $^{13}\text{C}$ -detected  $^1\text{H}$ -spin diffusion MAOSS NMR spectra of  $[\text{U-}^{13}\text{C}]$ -zervamicin/POPC (upper panel) and pure POPC membrane (lower panel). Both spectra were recorded at 298 K and with a spin diffusion mixing time of 145 ms. Connectivities are shown between the signals of lipid and water protons ( $y$ -axis) and the peaks of the  $^{13}\text{C}$  peptide atoms ( $x$ -axis). The residual cross peaks shown at the lower spectrum indicate a non-selective transfer of magnetization. The absence of correlations between 60, 180 ppm regions in the  $^{13}\text{C}$ -domain and 1, 3.4 ppm regions in the  $^1\text{H}$ -domain of the lower spectrum that the lipid  $^{13}\text{C}$ -signals are completely removed.

to optimize the signal to noise ratio. Figure 4 shows that the cross peaks at the 170–180 ppm, 52–73 ppm and 10–20 ppm  $^{13}\text{C}$ -regions correspond to amide,  $\text{C}^\alpha$  and aliphatic carbon atoms of the peptide (the weak cross peaks at the aromatic region are at the noise level). The selective detection of peptide signals is demonstrated by the spectrum of pure POPC membranes in the lower panel of Figure 4. The absence of signals in the lipid ester and lipid headgroup regions of the latter spectrum indicates that most of the  $^{13}\text{C}$  resonances shown in the upper panel belong to peptide signals (except for the region of 18–30 ppm, wherein overlapping signals of aliphatic peptide, lipid and polymer carbon atoms are still visible). Thus, under MAOSS conditions typical peptide signals can be observed at the carbonyl, alpha and aliphatic spectral regions without overlap with peaks of the lipid. The complete suppression of the lipid signals is achieved (due to the fast molecular motions of

the lipid molecules) by the combined affects of the  $T_2$  filter and the short contact time (156  $\mu\text{s}$ ) used during the cross polarization step.

It should be noted that the peaks at 53–70 ppm fall in the same region as were found for the  $\text{C}^\alpha$  signals of zervamicin in solution as well as in the micellar bound state (Balashova et al., 2002; Shenkarev et al., 2002). The peak at 70 ppm is easily assigned to overlapping signals of  $\beta$ -Thr<sup>6</sup> and  $\gamma$ -Hyp<sup>10,13</sup> carbon atoms.

Next, 2D-spectra of labelled zervamicin/POPC were recorded for different spin diffusion mixing times. As expected, the intensities of the different peaks shown at the  $^{13}\text{C}$  cross-sections decrease at shorter spin diffusion times. The build-up curves shown in Figure 5 were collected from  $^{13}\text{C}$  cross-sections at 1.0 ppm ( $\text{CH}_3$ - $\omega$ ) and 3.4 ppm (choline methyl). Careful inspection of the  $\text{C}^\alpha$  region for different traces showed the increase of the total integral at longer spin diffusion mixing times, but without local intensity changes for any of the individual partly overlapping peaks. This allowed us to determine the ‘intensity’ more accurately by integration of all peaks within the  $\text{C}^\alpha$  (53–68 ppm) region. The increase of the intensity at longer spin diffusion times was corrected with a factor  $\exp(\tau_m/T_1)$  to compensate for the decrease of intensity due to  $T_1$  relaxation. In Figure 5 the intensities were plotted as a function of the square root of the spin diffusion times in the same way as was earlier reported for the colicin channel protein (Huster et al., 2002). The build-up of the peptide-detected  $^1\text{H}$ - $\omega$ -methyl spin diffusion ( $\tau_{1/2} = 28.1$  ms) appears to be significantly slower than for the peptide detected  $^1\text{H}$ -choline curve ( $\tau_{1/2} = 7.8$  ms). It should be noted that these magnetization build-up rates are much faster than those reported for the colicin protein channel. However, the latter results were obtained different conditions, i.e. vesicular membranes, composed of a mixture of lipids, one partially deuterated.

Since the rate limiting step of the proton spin diffusion is related to distances, the distances between the  $\omega$ -methyl POPC and peptide protons are obviously larger compared to those between choline and peptide protons. In other words, the protons of the peptide are closer to the protons of the lipid head groups than to the deeply buried  $\omega$ -methyl lipid protons. Thus, the relatively slow build-up of the  $\omega$ -methyl signal is in line with a



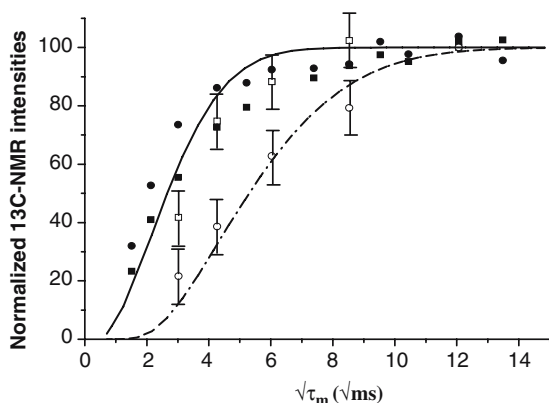


Figure 5. Build-up curves for  $^1\text{H}$ -spin diffusion rates of the transfer of  $^1\text{H}$ -magnetization of either ● choline methyl of PC10, ■  $\omega$ -methyl of PC10, □ choline methyl of POPC, or ○  $\omega$ -methyl protons of POPC to peptide protons and detected at the  $^{13}\text{C}$ -NMR domain. Normalized intensities of the  $\text{C}^\alpha$ -signals (53–68 ppm) of the peptide (see Materials and methods section) were plotted as a function of the root square of the spin diffusion mixing time  $\tau_m$  (in  $\sqrt{\text{ms}}$ ). Solid and broken lines were calculated on the basis of the 1D-lattice model described in (Huster et al., 2002).

peptide that is bound parallel to the surface of the thick POPC membrane.

The 2D  $^{13}\text{C}$ -detected  $^1\text{H}$ -spin diffusion-MAOSS-NMR spectrum of labelled zervamicin bound to thin PC10 membranes (not shown) appears to be very similar to the spectrum shown for this peptide bound to POPC. The control spectrum of pure lipid does not show any residual cross peaks at the  $\text{C}^\alpha$  region, demonstrating an efficient suppression of the choline proton peaks at this region of the spectrum. Build-up curves, shown in Figure 5, were obtained in the same manner as described for the spectrum of labelled zervamicin/POPC. For zervamicin/PC10, however, the rate of spin diffusion appears to be relatively rapid for lipid protons located at the surface (choline methyl) as well as for protons at the interior of the double layer ( $\omega$ -methyl). At this point it should be noted that in this membrane system zervamicin molecules are expected to be transmembrane oriented and the length of the peptide helix should span the thickness of the double layer. Indeed, the similar (and relatively fast) build-up curves shown for lipid protons at the interior and at the surface of the bilayer can be easily understood if there are similar (short) distances between these different lipid protons and the aliphatic side chains at the middle and at the termini of the peptide helix.

## Discussion and conclusions

Our experiments demonstrate a new method to prepare oriented bilayers with a high degree of lipid alignments that can be used to study the structure of peptide and proteins as well as their interaction with lipids at atomic resolution by  $^{13}\text{C}$ -NMR measurements. This was achieved by first loading the surface of a simple house hold foil with lipid, followed by hydration of the phospholipid and rolling this membrane loaded film to a cylinder of a diameter of 3 mm, prior to the insertion into a 4 mm rotor. The cheap 20  $\mu\text{m}$  thin foil, generally used to wrap up food, can be obtained at any local super market. For our purpose, it appears to be resistant to many organic solvents, including methanol, trifluoroethanol and ethyl acetate, which solvents are usually applied to load lipid/peptide mixtures on the surface of the substrate. The low weight to surface ratio of this film (40 mg lipid + 16 mg polymer/40  $\text{cm}^2$ ) allows measurements at high spinning speeds up to 11 kHz. For comparison, the total weight of the glass plates is approximately 534 mg/40  $\text{cm}^2$ , which restricts the spinning to much lower speeds. Thus, the increased stability of membranes at high spinning speeds is an important improvement to increase the sensitivity of the measurement by elimination of the spinning side bands which appear in the  $^{13}\text{C}$  spectra recorded at ultra-high field spectrometers due to chemical shift and dipolar anisotropies.

The surface of this flexible foil material is hydrophilic due to the manufacturing process of this co-polymer of ethylene and butene (3:1) to which 0.02% of glycerol monooleate is added to increase the wettability. In our preparations of oriented bilayers composed of 40 mg lipid allowed us to measure  $^{13}\text{C}$ -NMR spectra of peptide at molar ratios (P:L) varying between 1:53 and 1:70. After the drop-wise addition of the solution of the lipid-peptide mixture and subsequent evaporation of the solvent, the bilayers were hydrated by exposing the membrane loaded film with a fine mist of water (or buffer). In contrast to the long procedures reported in the literature, this fully reproducible method of hydration is easy and fast. It is even possible to hydrate the lipid by addition of a small drop of water directly inside the rotor containing the non-hydrated rolled film. However, measurements of intact membranes below the



freezing point of water are not possible in this case a very broad line appears in the  $^{31}\text{P}$ -NMR spectrum and the resolution of spinning side bands (which are observed at higher temperatures) was lost, indicating that lipids are not ordered at this condition. At higher temperatures, however, the method allows to study membranes composed of lipids in the liquid crystal state. If we assume that a lipid molecule occupies  $7.0\text{ nm}^2$  of the bilayer surface the calculated number of bilayers, separated by thin layers of water, is of the order of  $2 \times 10^5$ .

The utility of the new method to prepare samples of  $^{13}\text{C}$ -labelled peptides and proteins in well ordered membranes and in combination with the application of advanced 2D pulse schemes to obtain information at the molecular level is further demonstrated by the  $^{13}\text{C}$ -detected  $^1\text{H}$ -spin diffusion experiment. This experiment allowed us to separate the  $^{13}\text{C}$  signals of peptide from the overlapping natural abundance lipid peaks (Figure 4) and to measure the build-up curves. Qualitative analysis of these curves made it possible to distinguish the two different binding modes of zervamicin in terms of transmembrane and surface bound topologies in thin and thick membranes, respectively. Thus the results obtained are fully consistent with the previously reported results of the glass plate/membrane/zervamicin system, supporting the validity of this new foil-supported membrane system to study the phenomenon of the hydrophobic matching between a transmembrane peptide and the thickness of the membrane. The well-ordered substrate supported membrane system might also pave the way for studying the structure of peptides or proteins and the interaction with lipids at the atomic  $^{13}\text{C}$  level.

### Acknowledgements

We are grateful to Dr A.A. Tagaev and Dr T.I. Kostromina (Shemyakin-Ovchinnikov Institute of Bioorganic Chemistry, Moscow, Russia) for their contribution to the preparation of  $[\text{U-}^{13}\text{C}]$ -labelled zervamicin IIB. We thank Prof Dr Mei Hong for providing the spin diffusion simulation program and Dr Xiaolan Yao for her helpful hints to use

this program. This work was granted by the Netherlands Organisation for Scientific Research (NWO No. 047.014.017).

### References

- Agarwala, S., Mellor, I.P., Sansom, M.S.P., Karle, I.L., Flippen-Anderson, J.L., Uma, K., Krishna, K., Sukumar, M. and Balaram, P. (1992) *Biochem. Biophys. Res. Com.*, **186**, 8–15.
- Balaram, P., Krishna, K., Sukumar, M., Mellor, I.R. and Sansom, M.S.P. (1992) *Eur. Biophys. J.*, **21**, 117–128.
- Balashova, T.A., Shenkarev, Z.O., Tagaev, A.A., Ovchinnikova, T.V., Raap, J. and Arseniev, A.S. (2002) *FEBS Lett.*, **466**, 333–336.
- Bechinger, B., Aisenbrey, C., Sizun, C. and Harzer, U. (2001) In *Perspectives on Solid State NMR in Biology*, Kiihne, S.R. and de Groot, H.J.M. (Eds.), Kluwer, Dordrecht, pp. 45–53.
- Bechinger, B., Skladnev, D.A., Ogrel, A., Li, X., Rogozhkina, E.V., Ovchinnikova, T.V., O'Neil, J.D.J. and Raap, J. (2001) *Biochemistry*, **40**, 9428–9437.
- Eden, M. and Levitt, M.H. (1998) *J. Magn. Reson.*, **132**, 220–239.
- Forbes, J.C., Husted, C. and Oldfield, E. (1988) *J. Am. Chem. Soc.*, **110**, 1059–1065.
- Gaede, H.C. and Gawrisch, K. (2004) *Magn. Reson. Chem.*, **42**, 115–122.
- Glaubitx, C. and Watts, A. (1998) *J. Magn. Res.*, **130**, 305–316.
- Glaubitx, C. (2000) *Concepts Magn. Res.*, **12**, 137–151.
- Goldman, M. and Shen, L. (1966) *Phys. Rev.*, **144**, 321.
- Halladay, H.N., Stark, R.E., Ali, S. and Bittman, R. (1990) *Biophys. J.*, **58**, 1449–1461.
- Huster, D., Yao, X. and Hong, M. (2002) *J. Am. Chem. Soc.*, **124**, 874–883.
- Krishna, K., Sukumar, M. and Balaram, P. (1990) *Pure Appl. Chem.*, **62**, 1417–1420.
- Kumashiro, K.K., Schmidt-Rohr, K., Murphy, O.J. III, Ouellette, K.L., Cramer, W.A. and Thompson, L.K. (1998) *J. Am. Chem. Soc.*, **120**, 5043–5051.
- Marassi, F.M., Ramamoorthy, A. and Opella, S.J. (1997) *Proc. Natl. Acad. Sci. USA*, **94**, 8551–8556.
- Ovchinnikova, T.V., Shenkarev, Z.O., Yakimenko, S.A., Svishcheva, N.V., Tagaev, A.A., Skladnev, D.A. and Arseniev, A.S. (2003) *J. Pept. Sci.*, **9**, 817–826.
- Sansom, M.S.P., Balaram, P. and Karle, I.L. (1993) *Eur. Biophys. J.*, **21**, 369–383.
- Shenkarev, Z.O., Balashova, T.A., Efremov, R.G., Yakimenko, Z.A., Ovchinnikova, T.V. and Raap, J. (2002) *Biophys. J.*, **82**, 762–771.
- Sizun, C. and Bechinger, B. (2002) *J. Am. Chem. Soc.*, **124**, 1146.
- Smirnov, A.I. and Poluektov, O.G. (2003) *J. Am. Chem. Soc.*, **125**, 8434–8435.
- Wattaint, O. and Sarazin, C. (2005) *Biochim. Biophys. Acta*, **1713**, 65–72.